Journal of Zhejiang University-SCIENCE A (Applied Physics & Engineering)
ISSN 1673-565X (Print); ISSN 1862-1775 (Online)
www.zju.edu.cn/jzus; www.springerlink.com
E-mail: jzus@zju.edu.cn

Carrier distribution and electromechanical fields in a free piezoelectric semiconductor rod*

Chun-li ZHANG[1,3,4], Xiao-yuan WANG[1], Wei-qiu CHEN[1,3,4], Jia-shi YANG†‡[1,2]

([1]*Department of Engineering Mechanics, Zhejiang University, Hangzhou 310027, China*)

([2]*Department of Mechanical and Materials Engineering, University of Nebraska-Lincoln, Lincoln, NE 68588-0526, USA*)

([3]*Soft Matter Research Center, Zhejiang University, Hangzhou 310027, China*)

([4]*Key Laboratory of Soft Machines and Smart Devices of Zhejiang Province, Hangzhou 310027, China*)

†E-mail: jyang1@unl.edu

Received July 27, 2015; Revision accepted Oct. 26, 2015; Crosschecked Dec. 11, 2015

Abstract: We made a theoretical study of the carrier distribution and electromechanical fields in a free piezoelectric semiconductor rod of crystals of class 6 mm. Simple analytical expressions for the carrier distribution, electric potential, electric field, electric displacement, mechanical displacement, stress, and strain were obtained from a 1D nonlinear model reduced from the 3D equations for piezoelectric semiconductors. The distribution and fields were found to be either symmetric or antisymmetric about the center of the rod. They are qualitatively the same for electrons and holes. Numerical calculations show that the carrier distribution and the fields are relatively strong near the ends of the rod than in its central part. They are sensitive to the value of the carrier density near the ends of the rod.

Key words: Piezoelectricity, Semiconductor, Rod, Carrier distribution
http://dx.doi.org/10.1631/jzus.A1500213 **CLC number:** O33; TB1

1 Introduction

Piezoelectric materials are widely used to make electromechanical transducers for converting electric energy to mechanical energy or vice versa, and acoustic wave devices for frequency operation and sensing. In most cases, piezoelectric crystals and ceramics are treated as non-conducting dielectrics, but in reality there is no sharp division separating conductors from dielectrics. Real materials always show some conductance (Tiersten and Sham, 1998). For example, in acoustic wave devices made from quartz crystals, the small ohmic conductance and the related dissipative effects need to be considered when calculating the Q value (quality factor) of the devices (Lee *et al*., 2004; Yong *et al*., 2010; Wang *et al*., 2011), because other dissipative effects in quartz, such as material damping and radiation damping, are very small. Another origin of conduction in piezoelectric crystals is that some of them are in fact semiconductors with charge carriers of electrons and/or holes (Auld, 1973), e.g., the widely used ZnO and AlN films and fibers. In these materials, in addition to carrier drift under an electric field, carrier diffusion also contributes to the electric current. Piezoelectric semiconductors have been used to make devices for acoustic wave amplification (White, 1962; Yang and Zhou, 2004; Ghosh, 2006; Willatzen and Christensen, 2014) and acoustic charge transport (Schülein *et al*., 2013; Büyükköse *et al*., 2014) based on the acoustoelectric effect, i.e., the motion of carriers under the electric field produced by an acoustic wave through piezoelectric coupling. Recently, the electric field produced by mechanical fields in a piezoelectric semiconductor has been used to manipulate

‡ Corresponding author

* Project supported by the National Natural Science Foundation of China (Nos. 11202182, 11272281, and 11321202)

ORCID: Chun-li ZHANG, http://orcid.org/0000-0002-6688-2785; Jia-shi YANG, http://orcid.org/0000-0003-3971-1240

the operation of semiconductor devices, which forms the foundation of piezotronics (Wang *et al*., 2006; Wang, 2007; 2010). Piezoelectric semiconductors, such as ZnO, are also used for mechanical energy harvesting and conversion to electric energy (Hiralal *et al*., 2012; Kumar and Kim, 2012; Graton *et al*., 2013; Yin *et al*., 2013).

The basic behaviors of piezoelectric semiconductors can be described by the conventional theory which consists of the equations of linear piezoelectricity and the equations for the conservation of charges of electrons and holes (Hutson and White, 1962). This theory has been used to study some of the applications mentioned above: the inclusion problem for composites (Yang *et al*., 2006), the fracture of piezoelectric semiconductors (Hu *et al*., 2007; Sladek *et al*., 2014a; 2014b), the electromechanical energy conversion in these materials (Li *et al*., 2015), the vibrations of plates (Wauer and Suherman, 1997), and to develop low-dimensional theories of piezoelectric semiconductor plates and shells (Yang and Zhou, 2005; Yang *et al*., 2005). Researchers have also developed more general and fully nonlinear theories (de Lorenzi and Tiersten, 1975; McCarthy and Tiersten, 1978; Maugin and Daher, 1986).

This paper is concerned with the carrier distribution and electromechanical fields in the thin piezoelectric semiconductor rod, which is often used in piezoelectric semiconductor devices. The rod is free from externally applied mechanical and electrical loads. Because of the presence of carriers and the electromechanical coupling in the material, electromechanical fields develop and the carriers assume a certain spatial distribution. This problem is fundamental to the applications of piezoelectric semiconductor rods or wires. However, there exists some nonlinearity associated with the drift current, which is proportional to the product of the unknown carrier density and the unknown electric field (Pierret, 1988), and hence the problem presents some mathematical challenges. We performed a theoretical analysis using a 1D model and obtained simple and useful results for carrier distribution and electromechanical fields.

2 Equations for piezoelectric semiconductors

For a piezoelectric semiconductor, the 3D phenomenological theory consists of the linear momentum equation of motion, the charge equation of electrostatics, and the conservation of charge for electrons and holes (continuity equations) (Hutson and White, 1962; Pierret, 1988):

$$\begin{aligned} &T_{ji,j}=\rho\ddot{u}_i,\\ &D_{i,i}=q(p-n+N_D^+-N_A^-),\\ &J_{i,i}^n=q\dot{n},\\ &J_{i,i}^p=-q\dot{p}, \end{aligned} \tag{1}$$

where T_{ji} is the component of stress, ρ the mass density, u_i the component of mechanical displacement, D_i the component of electric displacement, q=1.6 $\times10^{-19}$ C the magnitude of the electronic charge, p and n the number densities of holes and electrons, N_D^+ and N_A^- the densities of impurities of donors and accepters, and J_i^p and J_i^n the hole and electron current densities, respectively. The reference state is the state before doping when the charges are not present. When the charges are introduced, they assume certain distributions and electromechanical fields develop. In Eq. (1), we have neglected carrier recombination and generation. Cartesian tensor notation has been used. A comma followed by an index indicates a partial derivative with respect to the coordinate associated with the index. A superimposed dot represents a time derivative. We consider doped n-type semiconductors for which n and N_D^+ are much greater than p and N_A^-. Therefore, we neglect p and N_A^- in this paper. In this case Eq. $(1)_{1\text{-}3}$ become uncoupled to the p in Eq. $(1)_4$. Constitutive relations for Eq. $(1)_{1\text{-}3}$ describing material behaviors can be written in the following form:

$$\begin{aligned} &S_{ij}=s_{ijkl}^E T_{kl}+d_{kij}E_k,\\ &D_i=d_{ikl}T_{kl}+\varepsilon_{ik}^T E_k,\\ &J_i^n=qn\mu_{ij}E_j+qD_{ij}n_{,j}, \end{aligned} \tag{2}$$

where S_{ij} is the component of strain, E_i the component of electric field, s_{ijkl}^E the elastic compliance constant, d_{kij} the piezoelectric constants, ε_{ij}^T the dielectric constant, μ_{ij} the carrier mobility, and D_{ij} the carrier diffusion constants. The superscripts "E" and

"T" in s^E_{ijkl} and ε^T_{ij} as well as the superscript "n" in J^n_i will be dropped in the rest of the paper. The strain S_{ij} and the electric field E_i are related to the mechanical displacement u_i and the electric potential ϕ through

$$\begin{aligned} S_{ij} &= \frac{1}{2}(u_{i,j} + u_{j,i}), \\ E_j &= -\phi_{,j}. \end{aligned} \tag{3}$$

3 1D model for a rod

Specifically, we consider a cylindrical rod of length $2L$ as shown in Fig. 1. It is within $|x_3|<L$. The cross section of the rod is arbitrary. Its surface is traction free. The rod is made from crystals of class 6 mm which includes the widely used crystals of ZnO and AlN. The c-axis of the crystal is along the axis of the rod, i.e., the x_3 axis. The rod is assumed to be long and thin. The electric field in the surrounding free space is neglected. The rod has electrons described by its density n varying along x_3 only. The electric field produced by the electrons causes deformation in the rod through piezoelectric coupling.

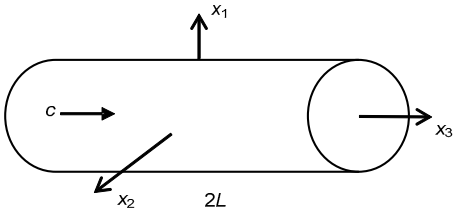

Fig. 1 A piezoelectric semiconductor rod of crystals of class 6 mm

The deformation of the thin rod is mainly an axial extension or contraction which can be described by a 1D model (Yang, 2005). For the 1D model, corresponding to Eq. $(1)_{1\text{-}3}$, the field equations for the static case we want to consider when all the time derivatives vanish are

$$\begin{aligned} &T_{33,3} = 0, \\ &D_{3,3} = q(-n + N_D^+), \\ &J_{3,3} = 0. \end{aligned} \tag{4}$$

For a thin rod, as will be seen later, the electrons tend to concentrate near the two ends of the rod. If the impurity is essentially uniform along the rod, then, near the two ends of the rod, which is the region of interest, n is much larger than N_D^+. Therefore, in the following we will neglect the non-mobile impurity charge N_D^+ in Eq. (4) and focus on the mobile electrons described by n. In the compact matrix notation (Yang, 2005), the relevant constitutive relations from Eq. (2) for the axial fields are

$$\begin{aligned} S_3 &= s_{33}T_3 + d_{33}E_3, \\ D_3 &= d_{33}T_3 + \varepsilon_{33}E_3, \\ J_3 &= qn\mu_{33}E_3 + qD_{33}n_{,3}. \end{aligned} \tag{5}$$

The relevant strain-displacement relation and the electric field-potential relation are the following ones from Eq. (3):

$$\begin{aligned} S_3 &= u_{3,3}, \\ E_3 &= -\phi_{,3}. \end{aligned} \tag{6}$$

Eq. $(5)_{1,2}$ can be solved for T_3 and rewritten as

$$\begin{aligned} T_3 &= \bar{c}_{33}S_3 - \bar{e}_{33}E_3, \\ D_3 &= \bar{e}_{33}S_3 + \bar{\varepsilon}_{33}E_3, \end{aligned} \tag{7}$$

where the effective 1D elastic, piezoelectric, and dielectric constants are:

$$\begin{aligned} \bar{c}_{33} &= 1/s_{33}, \\ \bar{e}_{33} &= d_{33}/s_{33}, \\ \bar{\varepsilon}_{33} &= \varepsilon_{33} - d_{33}^2/s_{33}. \end{aligned} \tag{8}$$

With the use of Eq. (6), Eqs. (7) and $(5)_3$ become:

$$\begin{aligned} T_3 &= \bar{c}_{33}u_{3,3} + \bar{e}_{33}\phi_{,3}, \\ D_3 &= \bar{e}_{33}u_{3,3} - \bar{\varepsilon}_{33}\phi_{,3}, \\ J_3 &= -qn\mu_{33}\phi_{,3} + qD_{33}n_{,3}, \end{aligned} \tag{9}$$

which are the 1D constitutive relations ready to be used in Eq. (4).

4 Carrier distribution and fields

The substitution of Eq. $(9)_{1,2}$ in Eq. $(4)_{1,2}$ yields

$$\begin{aligned} &\bar{c}_{33}u_{3,33}+\bar{e}_{33}\phi_{,33}=0,\\ &\bar{e}_{33}u_{3,33}-\bar{\varepsilon}_{33}\phi_{,33}=-qn, \end{aligned} \tag{10}$$

which can be rearranged to

$$\begin{aligned} u_{3,33}&=-\frac{\bar{e}_{33}}{\bar{c}_{33}}\phi_{,33},\\ n&=\frac{\varepsilon_{33}}{q}\phi_{,33}. \end{aligned} \tag{11}$$

Eq. $(4)_3$ can be integrated to give

$$J_3=-qn\mu_{33}\phi_{,3}+qD_{33}n_{,3}=C_1\varepsilon_{33}, \tag{12}$$

where Eq. $(9)_3$ has been used and C_1 is an integration constant. Substituting Eq. $(11)_2$ into Eq. (12), we can obtain

$$-\mu_{33}\phi_{,33}\phi_{,3}+D_{33}\phi_{,333}=C_1. \tag{13}$$

The integration of Eq. (13) leads to

$$-\frac{1}{2}\mu_{33}(\phi_{,3})^2+D_{33}\phi_{,33}=C_1x_3+C_2D_{33}, \tag{14}$$

where C_2 is another integration constant. Let

$$-\phi_{,3}=E_3=E, \tag{15}$$

then Eq. (14) takes the following form

$$-\frac{1}{2}\mu_{33}E^2-D_{33}E_{,3}=C_1x_3+C_2D_{33}. \tag{16}$$

For the static and free rod we are considering, J_3=0 and hence C_1=0. Eq. (16) reduces to

$$E_{,3}+aE^2=-b, \tag{17}$$

where we have denoted

$$a=\frac{1}{2}\frac{\mu_{33}}{D_{33}}=\frac{1}{2}\frac{q}{kT},\ b=C_2. \tag{18}$$

In Eq. (18), we have used the Einstein relationship (Navon, 1986) that

$$\frac{\mu_{33}}{D_{33}}=\frac{q}{kT}. \tag{19}$$

Since a>0, from Eq. (17) it can be seen that b>0 if $E_{,3}$<0 and dominates aE^2, which is always positive. In this case ab>0 and the solution to Eq. (17) can be found as

$$E=-\phi_{,3}=-\frac{b\tan\left[\sqrt{ab}\,(x_3-C_3)\right]}{\sqrt{ab}}, \tag{20}$$

where C_3 is an integration constant. Because of the symmetry in the problem, we expect that E=0 when x_3=0 which can be satisfied by choosing C_3=0 in Eq. (20). Then, integrating Eq. (20), we have

$$\phi=-\frac{1}{a}\ln\left[\cos(\sqrt{ab}\,x_3)\right]+C_4, \tag{21}$$

where C_4 is an integration constant and is immaterial. The substitution of Eq. (20) in Eq. $(11)_2$ gives the carrier distribution which is always positive:

$$n=\frac{\varepsilon_{33}}{q}\frac{b}{\cos^2(\sqrt{ab}\,x_3)}. \tag{22}$$

From Eqs. $(11)_1$ and (20), we can obtain

$$S_3=u_{3,3}=-\frac{\bar{e}_{33}}{\bar{c}_{33}}\frac{b\tan(\sqrt{ab}\,x_3)}{\sqrt{ab}}+C_5, \tag{23}$$

and

$$u_3=\frac{\bar{e}_{33}}{\bar{c}_{33}}\frac{1}{a}\ln\left[\cos(\sqrt{ab}\,x_3)\right]+C_5x_3+C_6, \tag{24}$$

where C_5 and C_6 are integration constants. C_6 represents a rigid-body displacement and can be set to zero. Then, from Eq. $(7)_1$,

$$T_3=\bar{c}_{33}C_5. \tag{25}$$

For a free rod without an axial force, C_5=0. From Eq. $(7)_2$,

$$D_3 = -\varepsilon_{33}\frac{b\tan(\sqrt{ab}\,x_3)}{\sqrt{ab}}. \tag{26}$$

In summary, the electromechanical fields and the carrier distribution are:

$$\begin{aligned}
&u_3 = \frac{\bar{e}_{33}}{\bar{c}_{33}}\frac{1}{a}\ln\left[\cos(\sqrt{ab}\,x_3)\right],\\
&S_3 = -\frac{\bar{e}_{33}}{\bar{c}_{33}}\frac{b\tan(\sqrt{ab}\,x_3)}{\sqrt{ab}},\\
&T_3 = 0,\\
&\phi = -\frac{1}{a}\ln\left[\cos(\sqrt{ab}\,x_3)\right],\\
&E_3 = -\frac{b\tan(\sqrt{ab}\,x_3)}{\sqrt{ab}},\\
&D_3 = -\varepsilon_{33}\frac{b\tan(\sqrt{ab}\,x_3)}{\sqrt{ab}},\\
&n = \frac{\varepsilon_{33}}{q}\frac{b}{\cos^2(\sqrt{ab}\,x_3)},\\
&J_3 = 0.
\end{aligned} \tag{27}$$

The traction-free mechanical end conditions are satisfied by T_3=0. The non-conducting end conditions are satisfied by J_3=0. b is related to C_2 through Eq. $(18)_2$ and is the only integration constant left. To determine b, we impose the boundary condition that the carrier density at the ends of the rod where x_3=L is known to be n_0 and

$$\frac{\varepsilon_{33}}{q}\frac{b}{\cos^2(\sqrt{ab}\,L)} = n_0. \tag{28}$$

n_0 makes the boundary value problem non-homogeneous and may be viewed as a driving term or a load.

In the case when holes dominate, Eqs. $(4)_2$ and $(5)_3$ should be replaced by (Pierret, 1988)

$$D_{3,3} = qp, \tag{29}$$

and

$$J_3 = qp\mu_{33}E_3 - qD_{33}p_{,3}. \tag{30}$$

In this case, formally Eq. (17) is still valid but a becomes negative. When b<0, if $E_{,3}$>0 and dominates aE^2 which is always negative, we still have ab>0 and the solution to Eq. (17) is still given by Eq. (20). Then the carrier distribution and the electromechanical fields are still given by Eq. (27). The only difference is that for holes a and b are both negative.

5 Numerical results and discussion

Denoting $X = \sqrt{ab}\,L$, we write Eq. (28) as the following equation for X:

$$\cos X = \pm gX, \tag{31}$$

where

$$g = \frac{1}{L}\sqrt{\frac{\varepsilon_{33}}{qan_0}}. \tag{32}$$

As a numerical example, consider a rod with L=10 mm. At room temperature kT/q=0.026 V (Pierret, 1988) which determines a through Eq. (18). The material constants for ZnO can be found in Auld (1973). For different values of n_0 and hence g, we plot Y=cos$X$ and Y=±gX in Fig. 2. The intersections of the two families of curves determine the roots of Eq. (31). When n_0=10^{12} m^{-3}, there is only one root. When n_0=10^{14} m^{-3}, there are several roots. When n_0 increases further, the slopes of the straight lines described by Y=±gX become smaller which implies more roots of Eq. (31). This is not surprising in view of the nonlinear nature of the problem which is associated with strong fields and high carrier density.

Fig. 3 shows the carrier distribution $n(x_3)$ along the rod for different values of n_0. For these values of n_0, there are multiple roots from Eq. (31). The first root is chosen which presents the physical picture expected. $n(x_3)$ is symmetric about the rod center as expected. $n(x_3)$ is nearly constant in the central part of the rod, and increases rapidly near the ends. When n_0 increases, the carrier density near the rod ends is more sensitive to n_0 than the carrier density in the central part. Later, more insight into the carrier distribution will be given when examining the electric field in the rod.

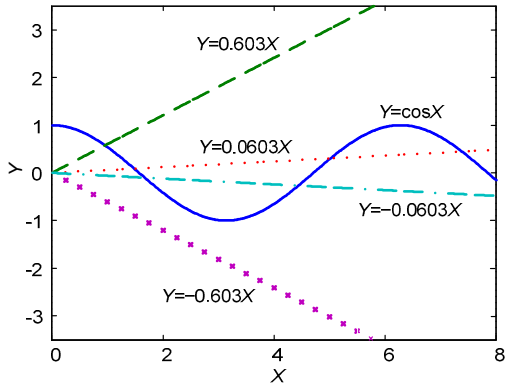

Fig. 2 Roots of Eq. (31): n_0=10^{12} m^{-3}, Y=±0.603X; n_0=10^{14} m^{-3}, Y=±0.0603X

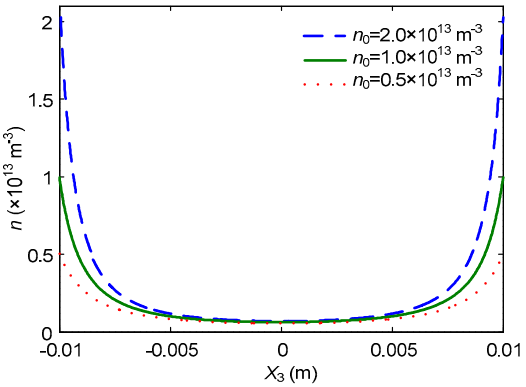

Fig. 3 Carrier distribution along the rod

Fig. 4 shows the axial distributions of the electric field E_3, the electric potential φ, and the electric displacement D_3. The electric field in Fig. 4a is physically symmetric about x_3=0 as it should be, but mathematically it is described by an odd function of x_3. As an odd function it vanishes at the origin. It increases its magnitude rapidly near the ends of the rod, which is consistent with the fact shown in Fig. 3 that near the ends the carrier distribution also has a large gradient. The electric field and the gradient of $n(x_3)$ have to balance each other to make J_3=0. Hence, E_3 and n_3 have to be large or small together in magnitude. A larger n_0 is associated with a higher electric field as expected. The electric potential in Fig. 4b is the spatial integration of E_3 along the rod and as a consequence it is an even function of x_3. It may have an arbitrary constant which is fixed by choosing $\varphi(0)$=0. A larger n_0 is also associated with a higher electric potential as expected. The behavior of D_3 in Fig. 4c is similar to that of E_3 in Fig. 4a.

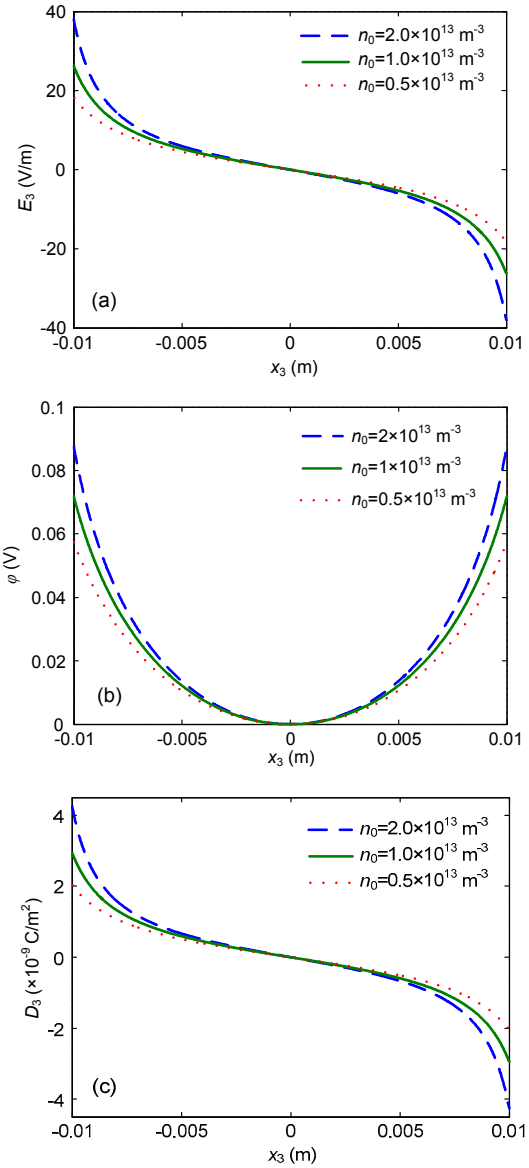

Fig. 4 Axial distributions of the electric field E_3 (a), electric potential φ (b), and electric displacement D_3 (c)

Fig. 5 shows the mechanical fields which are present because the material is piezoelectric. For free extension the axial stress is zero. Hence, only the axial strain and the axial displacement are plotted in Fig. 5a and Fig. 5b, respectively. The strain is an odd function of x_3, indicating that half of the rod is in axial extension and the other half in contraction. This is related to the fact that the electric field in Fig. 4a is also an odd function of x_3. For the displacement in Fig. 5b, the rigid-body axial displacement is removed by choosing the axial displacement at the rod center to be zero. From Fig. 5 it can be

seen that the mechanical fields are also relatively large near the ends of the rod and are sensitive to n_0 near the ends.

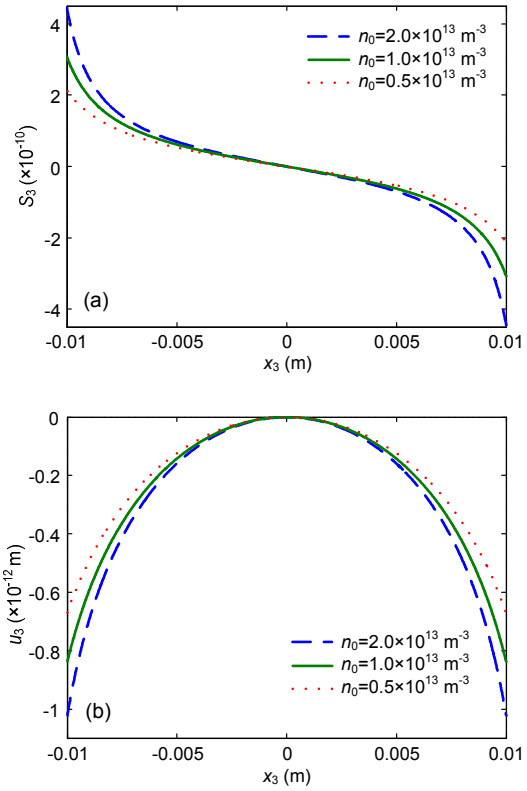

Fig. 5 Axial strain (a) and axial displacement (b)

6 Conclusions

Because of the presence of carriers and piezoelectric coupling, a thin piezoelectric semiconductor rod undergoes axial extension/contraction. The equations for determining the carrier density and electromechanical fields are nonlinear because of the drift current term. The carrier distribution and electromechanical fields are either symmetric or antisymmetric about the center of the rod. They are relatively strong near the ends of the rod than at its central part. They are also sensitive to the number of carriers. The effects of electrons and holes are qualitatively the same.

References

Auld, B.A., 1973. Acoustic Fields and Waves in Solids. John Wiley and Sons, New York, p.357-382.

Büyükköse, S., Hernández-Mínguez, A., Vratzov, B., *et al*., 2014. High-frequency acoustic charge transport in GaAs nanowires. *Nanotechnology*, **25**(13):135204. http://dx.doi.org/10.1088/0957-4484/25/13/135204

de Lorenzi, H.G., Tiersten, H.F., 1975. On the interaction of the electromagnetic field with heat conducting deformable semiconductors. *Journal of Mathematical Physics*, **16**(4):938-957. http://dx.doi.org/10.1063/1.522600

Ghosh, S.K., 2006. Acoustic wave amplification in ion-implanted piezoelectric semiconductor. *Indian Journal of Pure and Applied Physics*, **44**(2):183-187.

Graton, O., Poulin-Vittrant, G., Hue, L.T.H., *et al*., 2013. A strategy of modelling and simulation of electromechanical conversion in ZnO nanowires. *Advances in Applied Ceramics*, **112**(2):85-90. http://dx.doi.org/10.1179/1743676112Y.0000000029

Hiralal, P., Unalan, H.E., Amaratunga, G.A., 2012. Nanowires for energy generation. *Nanotechnology*, **23**(19):194002. http://dx.doi.org/10.1088/0957-4484/23/19/194002

Hu, Y.T., Zeng, Y., Yang, J.S., 2007. A mode III crack in a piezoelectric semiconductor of crystals with 6mm symmetry. *International Journal of Solids and Structures*, **44**(11-12):3928-3938. http://dx.doi.org/10.1016/j.ijsolstr.2006.10.033

Hutson, A.R., White, D.L., 1962. Elastic wave propagation in piezoelectric semiconductors. *Journal of Applied Physics*, **33**(1):40-47. http://dx.doi.org/10.1063/1.1728525

Kumar, B., Kim, S.W., 2012. Energy harvesting based on semiconducting piezoelectric ZnO nanostructures. *Nano Energy*, **1**(3):342-355. http://dx.doi.org/10.1016/j.nanoen.2012.02.001

Lee, P.C.Y., Liu, N.H., Ballato, A., 2004. Thickness vibrations of a piezoelectric plate with dissipation. *IEEE Transactions on Ultrasonics, Ferroelectrics and Frequency Control*, **51**(1):52-62. http://dx.doi.org/10.1109/TUFFC.2004.1268467

Li, P., Jin, F., Yang, J.S., 2015. Effects of semiconduction on electromechanical energy conversion in piezoelectrics. *Smart Materials and Structures*, **24**(2):025021. http://dx.doi.org/10.1088/0964-1726/24/2/025021

Maugin, G., Daher, N., 1986. Phenomenological theory of elastic semiconductors. *International Journal of Engineering Science*, **24**(5):703-731. http://dx.doi.org/10.1016/0020-7225(86)90106-0

McCarthy, M.F., Tiersten, H.F., 1978. On integral forms of the balance laws for deformable semiconductors. *Archive for Rational Mechanics and Analysis*, **68**(1):27-36. http://dx.doi.org/10.1007/BF00276177

Navon, D.H., 1986. Semiconductor Microdevices and Materials. CBS College Publishing, New York.

Pierret, R.F., 1988. Semiconductor Fundamentals, 2nd Edition. Addison-Wesley, Reading, Massachusetts, USA.

Schülein, F.J.R., Müller, K., Bichler, M., *et al*., 2013. Acoustically regulated carrier injection into a single

optically active quantum dot. *Physical Review B*, **88**(8): 085307.
http://dx.doi.org/10.1103/PhysRevB.88.085307

Sladek, J., Sladek, V., Pan, E.N., *et al*., 2014a. Dynamic anti-plane crack analysis in functional graded piezoelectric semiconductor crystals. *CMES: Computer Modeling in Engineering & Sciences*, **99**(4):273-296.
http://dx.doi.org/10.3970/cmes.2014.099.273

Sladek, J., Sladek, V., Pan, E.N., *et al*., 2014b. Fracture analysis in piezoelectric semiconductors under a thermal load. *Engineering Fracture Mechanics*, **126**:27-39.
http://dx.doi.org/10.1016/j.engfracmech.2014.05.011

Tiersten, H.F., Sham, T.L., 1998. On the necessity of including electrical conductivity in the description of piezoelectric fracture in real materials. *IEEE Transactions on Ultrasonics, Ferroelectrics and Frequency Control*, **45**(1):1-3.
http://dx.doi.org/10.1109/58.646895

Wang, J., Zhao, W.H., Du, J.K., *et al*., 2011. The calculation of electrical parameters of AT-cut quartz crystal resonators with the consideration of material viscosity. *Ultrasonics*, **51**(1):65-70.
http://dx.doi.org/10.1016/j.ultras.2010.05.009

Wang, X.D., Zhou, J., Song, J.H., *et al*., 2006. Piezoelectric field effect transistor and nanoforce sensor based on a single ZnO nanowire. *Nano Letters*, **6**(12):2768-2772.
http://dx.doi.org/10.1021/nl061802g

Wang, Z.L., 2007. Nanopiezotronics. *Advanced Materials*, **19**(6):889-892.
http://dx.doi.org/10.1002/adma.200602918

Wang, Z.L., 2010. Piezopotential gated nanowire devices: piezotronics and piezo-phototronics. *Nano Today*, **5**(6): 540-552.
http://dx.doi.org/10.1016/j.nantod.2010.10.008

Wauer, J., Suherman, S., 1997. Thickness vibrations of a piezo-semiconducting plate layer. *International Journal of Engineering Science*, **35**(15):1387-1404.
http://dx.doi.org/10.1016/S0020-7225(97)00060-8

White, D.L., 1962. Amplification of ultrasonic waves in piezoelectric semiconductors. *Journal of Applied Physics*, **33**(8):2547-2554.
http://dx.doi.org/10.1063/1.1729015

Willatzen, M., Christensen, J., 2014. Acoustic gain in piezoelectric semiconductors at ϵ-near-zero response. *Physical Review B*, **89**(4):041201.
http://dx.doi.org/10.1103/PhysRevB.89.041201

Yang, J.S., 2005. An Introduction to the Theory of Piezoelectricity. Springer, Berlin.

Yang, J.S., Zhou, H.G., 2004. Acoustoelectric amplification of piezoelectric surface waves. *Acta Mechanica*, **172**(1-2):113-122.
http://dx.doi.org/10.1007/s00707-004-0140-z

Yang, J.S., Zhou, H.G., 2005. Amplification of acoustic waves in piezoelectric semiconductor plates. *International Journal of Solids and Structures*, **42**(11-12):3171-3183.
http://dx.doi.org/10.1016/j.ijsolstr.2004.10.011

Yang, J.S., Yang, X.M., Turner, J.A., 2005. Amplification of acoustic waves in piezoelectric semiconductor shells. *Journal of Intelligent Material Systems and Structures*, **16**(7-8):613-621.
http://dx.doi.org/10.1177/1045389X05051626

Yang, J.S., Song, Y.C., Soh, A.K., 2006. Analysis of a circular piezoelectric semiconductor embedded in a piezoelectric semiconductor substrate. *Archive of Applied Mechanics*, **76**(7-8):381-390.
http://dx.doi.org/10.1007/s00419-006-0035-7

Yin, K., Lin, H.Y., Cai, Q., *et al*., 2013. Silicon nanowires nanogenerator based on the piezoelectricity of alpha-quartz. *Nanoscale*, **5**(24):12330-12334.
http://dx.doi.org/10.1039/c3nr03838f

Yong, Y.K., Patel, M.S., Tanaka, M., 2010. Theory and experimental verifications of the resonator Q and equivalent electrical parameters due to viscoelastic and mounting supports losses. *IEEE Transactions on Ultrasonics, Ferroelectrics and Frequency Control*, **57**(8):1831-1839.
http://dx.doi.org/10.1109/TUFFC.2010.1622

中文概要

题　目： 压电半导体杆中的机械场、电场与载流子分布研究

目　的： 导出两端自由压电半导体杆在自平衡状态下内部的位移、电场和载流子的解析表达式，研究它们在杆内的分布规律。

方　法： 从三维压电半导体基本方程出发，以 n-型半导体为例，导出考虑拉伸变形模式的一维模型方程。由平衡方程和电学高斯方程和平衡态下杆内电流为零的条件得到以电场为未知函数一阶非线性偏微分方程，再利用两端自由的边界条件解出位移、电场和载流子的分布函数。

结　论： 压电半导体杆内位移、载流子和电势关于杆的几何中心对称分布，电场、应变则关于中心呈反对称分布形式；它们在半导体两端部的区域变化比在中心区域的变化剧烈。此外，半导体杆两端部的载流子浓度、位移和电场显著依赖于端部的初始载流子浓度。

关键词： 力电耦合；半导体；杆；载流子